

Belo Horizonte, Brazil; September 09-14, 2018

# AN ACTIVE-PASSIVE NONLINEAR FINITE ELEMENT MODEL FOR ELECTROMECHANICAL COMPOSITE MORPHING BEAMS

Raul B. Olympio\*,\*\*, Mauricio V. Donadon\*, Saullo G. P. Castro\*\*
\*Instituto Tecnológico de Aeronáutica (ITA), \*\*EMBRAER S.A.

Keywords: nonlinear, finite element model, composite, piezoelectric, morphing

#### **Abstract**

The use of morphing structures aims to increase aerodynamic efficiency, decreasing fuel consumption and aircraft overall weight. Within this context, piezoelectric materials are of great interest in the design of smart structures because the piezoelectric effect is reversible, allowing them to work both as sensors and as actuators. The present work proposes a geometrically nonlinear finite element formulation for composite beams with embedded piezoelectric layers for application in morphing aerostructures. The formulation uses the complete Green strain tensor to account for geometric nonlinearities, and linear piezoelectricity to model the electromechanical behavior. A set of nonlinear equilibrium equations results from the application of variational principles, and is finally solved by means of an iterative-incremental arc length method. The sensitivity of the element to stacking sequence and number of actuators are investigated.

#### 1 Introduction

According to the Defense Advanced Research Projects Agency (DARPA), a morphing aircraft is an air vehicle capable of substantially changing its state and providing superior system capability by means of innovative technology integrated in its design. Early technologies involved in changing shape capability relied on heavy motors and complex hydraulic systems which lead to structural reinforcement and increase in weight, like the ones implemented in the F-14, F-111 and Tornado fighter aircrafts [1, 2]. In order to accommodate large structural changes and comply with overall weight requirements, researchers put some effort in the improvement of smart materials and their use as actuators. Shape memory alloys, piezoelectric and electrostrictive materials are promising candidates to replace conventional shape changing mechanism due to their notable energy density [1].

The use of macro fiber composites (MFC) to include morphing capabilities into structures became popular over the last decade [3, 4, 5]. MFC consists of unidirectional piezoelectric fibers, usually PZT-5A, within a polymer matrix, which is sandwiched between copper electrodes and Kapton film layers. This configuration allows the utilization of high piezoelectric coupling coefficient, concentrating the applied voltage inside the ceramic. The aforementioned smart actuator can be used in an elevon configuration [3], as flap-like structure [4] and as a replacement of the aileron section of a wing [5]. Due to the actuator light weight, flexibility and ability to respond rapidly to input voltage, the MFC is an interesting choice as morphing mechanism.

Another compelling characteristic of piezoelectric material is that the piezoelectric effect is reversible, which means this smart material can be used actively as an actuator or passively as a sensor [6]. Additionally, it can be embedded into a laminate in order to add sensing and actuating capabilities into the structure [7]. To analyze the voltage response in the case of sensors, and the displacement due to an applied electric potential in the case of actuators, a model that incorporates the electromechanical behavior of piezoelectric materials should be available. The finite element method is a versatile tool that can easily take these characteristics into account and combine them to an structural analysis software.

From 1988 to 1997 the number of papers on modeling smart structures using the finite element method increased more than seven times [8]. Early works were dedicated to model ultrasonic transducers, but recently the use of piezoelectric materials as active structures became more popular. The author presents a great deal of finite element formulations regarding its shape, order of approximation functions, nodal degrees of freedom, total degrees of freedom (DOF) and assumptions used to derive the element. Three dimensional solid elements were modeled using four-node tetrahedral and eight or twenty-node hexahedral elements with sixteen to a hundred DOF. Two dimensional plate elements were derived using three-node triangular and four, eight or ninenode quadrilateral elements, exhibiting between twelve to a hundred and four DOF. The one dimensional beam elements were modeled using two-node linear elements with eight or ten DOF.

Plates and beams formulations perform better than a solid element when analyzing thin structures [8]. However, one dimensional formulations have relatively less DOF decreasing computational cost while maintaining precision. Common beam models are based on Euler-Bernoulli [9] or Timoshenko [10, 11] theory. A comparison between finite element formulations using Euler-Bernoulli and Timoshenko beam theories is presented by Wang [9]. The fact that interpolation functions are the exact solutions of the governing equations of motion guarantees fast convergence with a

minimum number of elements. He concludes that the first formulation is accurate enough to predict the behavior of slender beams, with slenderness ratio greater than twenty. For lower ratios, the latter formulations should be used.

Kusculuoglu et al. [10] develop a unimorph piezoelectric actuator where the substrate and electromechanical materials have different cross-section rotations. Linear shape functions are used to interpolate the axial displacement and rotations, while a third degree polynomial is used for the transversal motion. Experiments and comparison with ANSYS<sup>(R)</sup> commercial finite element code were used to validate the model. With increasing thickness, shear effects and rotational inertia become more important and the model developed in their work predicts the beam behavior in a more accurate way.

Alaimo et al. [11] propose a two-node formulation for multi-layer composite smart beam in which the electrical degrees of freedom are condensed and the problem is treated only in the mechanical domain, with the electric response being available through algebraic manipulation. Timoshenko beam theory and quadratic through-thickness distribution of the electric potential are assumed. By using Hermite interpolation functions, the resulting element is superconvergent and does not present shear locking. The current model performance was compared with a two dimensional laminate modeled using COMSOL Multiphysics<sup>(R)</sup>. The results for a two-node, nine degree of freedom element matched the 81,153 DOF plate model very well, with substantially lower computational cost.

The effects of nonlinearities into the finite element formulation of piezoelectric structures were also studied [12]. The electromechanical coupling behavior is modeled using linear piezoelectricity. The formulation presented in their work is applicable to one, two or three dimensional elements, depending only on the choice of interpolation functions. In their sim-

ulations, serendipity eight node plate elements were used, with the same shape functions for displacement and electric potential. By using Newton-Raphson method associated with arc length constraints the authors show that this general nonlinear finite element model can predict well the structure behavior before and after limit points, which are pairs in the load-displacement space in which the tangent stiffness matrix becomes singular.

In this paper, a novel nonlinear finite element model for composite beams with embedded piezoelectric layers is developed. The geometric nonlinearity is added by means of the complete Green strain tensor, while the piezoelectric effect is modeled using the standard linear approximation. The formulation also takes into account the layerwise mechanical behavior of the beam. Voigt notation will be used throughout the text.

#### 2 Mathematical Formulation

A laminate beam with n layers, consisting of composite or piezoelectric materials, is considered. The beam has length L and rectangular cross section with width b and thickness h as seen in Fig. 1. The beam is considered to have  $n_a$  actuator and  $n_s$  sensor layers polarized in the thickness direction. Each layer has z-coordinates  $z_{n-1}$  and  $z_n$  as shown in Fig. 2.



Fig. 1: Beam element.

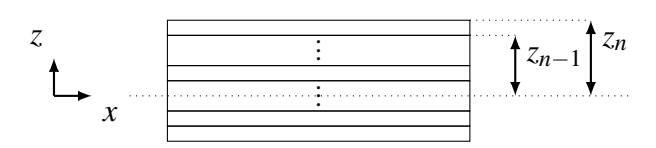


Fig. 2: Lateral view of a laminate.

#### 2.1 Basic Assumptions

For a composite unidirectional ply, the elastic constants are dependent on the fiber orientation. A usual coordinate system is defined as seem in Fig. 3, where the 1-direction coincides with the fiber, the 2-direction is perpendicular to the fibers, in the plane of the lamina and 3-direction is normal to the plane of the lamina. A laminate is constructed when various plies are assembled together. Due to the different orientations of each lamina, the stress-strain relationship of the laminate should be expressed in an arbitrary coordinate system (x, y, z).

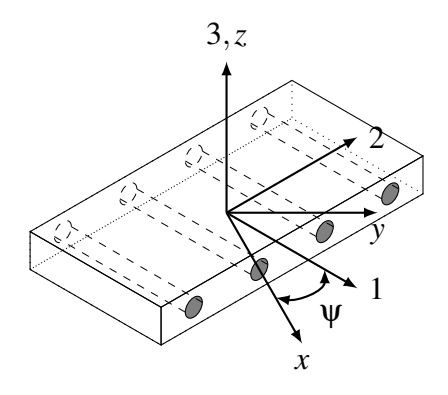


Fig. 3: Global (x, y, z) and local (1, 2, 3) coordinate systems.

The rotation of each lamina around the 3-direction gives the following mechanical constitutive relationship

$$\{\sigma\}_k = \left[\bar{Q}\right]_k \{\epsilon\}_k, \qquad k = 1, 2 \dots n \quad (1)$$

with  $\{\sigma\}_k = \{\sigma_{xx} \quad \sigma_{yy} \quad \sigma_{zz} \quad \tau_{yz} \quad \tau_{xz} \quad \tau_{xy} \}^T$  being the second order stress tensor represented in vector notation,  $\{\varepsilon\}_k = \{\varepsilon_{xx} \quad \varepsilon_{yy} \quad \varepsilon_{zz} \quad \gamma_{yz} \quad \gamma_{xz} \quad \gamma_{xy} \}^T$  the engineering strain vector and  $[\bar{Q}]_k$  the fourth order constitutive stiffness tensor represented in matrix form for the rotated laminate. This equivalent material properties matrix is given by

$$\left[\bar{Q}\right]_{k} = \left[T\right]_{k} \left[Q\right]_{k} \left[T\right]_{k}^{T} \tag{2}$$

where  $[Q]_k$  is constitutive stiffness matrix in the (1,2,3) coordinate system, and  $[T]_k$  is a

transformation matrix expressed as

with  $c = \cos \psi_k$  and  $s = \sin \psi_k$ .

The engineering strain vector considered in this work is derived from the complete Green strain tensor, which is defined as following using index notation

$$\varepsilon_{ij} = \frac{1}{2} \left( \frac{\partial u_i}{\partial x_j} + \frac{\partial u_j}{\partial x_i} + \frac{\partial u_k}{\partial x_i} \frac{\partial u_k}{\partial x_j} \right), \quad i, j, k = 1...3$$
(4)

with  $u_i$  being the components of displacement and  $x_i$  the directions of the global coordinate system. The engineering components of shear strain tensor are

$$\gamma_{ij} = 2\varepsilon_{ij}$$
, for  $i \neq j$ 

The constitutive relationships that dictates the electromechanical behavior of the piezoelectric layers are expressed as

$$\{\sigma\} = [Q]\{\epsilon\} - [e]\{E\}$$
  
$$\{D\} = [e]^T \{\epsilon\} + [\epsilon]^{\epsilon} \{E\}$$
 (5)

where [e] is a  $3 \times 6$  piezoelectric coefficient matrix and  $[\varepsilon]^{\varepsilon}$  is the dielectric permittivity at constant strain.  $\{D\}$  and  $\{E\}$  are the electric displacement and field vectors, respectively. Each element  $e_{ij}$  expresses the sensitivity of the piezoelectric material in the *i*-direction when a stimuli is applied in the *j*-direction and vice-versa. Equations 5 are used to model both actuator and sensor layers, respectively, and will be used in the rest of this work.

The kinematic relationships between displacements and strains follow from Timoshenko's beam theory. It states that after the application of load, the beam cross-sections remain plane and rigid, but not perpendicular

to the neutral axis. For a beam moving in the x-z plane, as seen in Fig. 4, the displacement field is given by

$$\bar{u} = u(x) - z \Theta(x)$$

$$\bar{v} = 0$$

$$\bar{w} = w(x)$$
(6)

where u and w are the axial and transversal displacements of the neutral axis, respectively, and  $\theta$  is the cross section rotation.

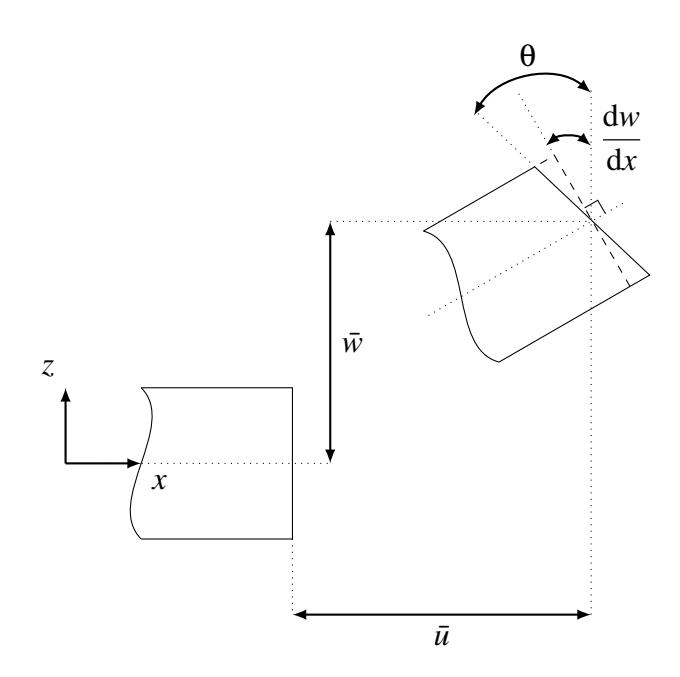


Fig. 4: Timoshenko's beam kinematic assumptions.

#### 2.2 Finite Element Method

In the finite element method, the displacement field in Equation (6) is expressed as a linear combination of shape functions and the nodal displacements. For this formulation, a beam with 3 equally spaced nodes, as the one in Fig. 5, is chosen. There are a total of 9 mechanical and  $n_s$  electrical DOFs for each element. To simplify the definition of shape functions, a natural coordinate system is defined as shown in Fig. 6. Writing the  $2^{nd}$ -order Lagrangian polynomials in the aforementioned coordinate system gives

# AN ACTIVE-PASSIVE NONLINEAR FINITE ELEMENT MODEL FOR ELECTROMECHANICAL COMPOSITE MORPHING BEAMS

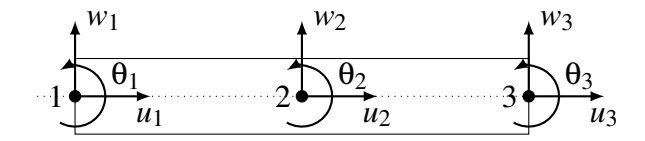


Fig. 5: 3-node beam element.

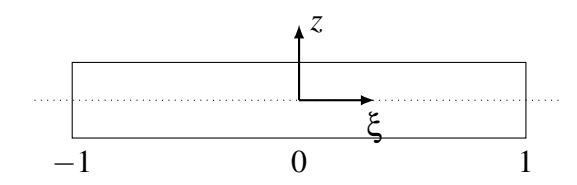


Fig. 6: Beam natural coordinate system.

$$N_1(\xi) = \frac{1}{2}\xi(\xi - 1)$$

$$N_2(\xi) = 1 - \xi^2$$

$$N_3(\xi) = \frac{1}{2}\xi(\xi + 1)$$
(7)

which allow the displacements to be written as

$$u = \{N_1 \quad N_2 \quad N_3\} \left\{ \begin{array}{c} u_1 \\ u_2 \\ u_3 \end{array} \right\}$$

$$w = \{N_1 \quad N_2 \quad N_3\} \left\{ \begin{array}{c} w_1 \\ w_2 \\ w_3 \end{array} \right\}$$

$$\theta = \{N_1 \quad N_2 \quad N_3\} \left\{ \begin{array}{c} \theta_1 \\ \theta_2 \\ \theta_3 \end{array} \right\}$$
(8)

Considering that the electric field is applied only in the thickness direction, and admitting that it varies linearly across the piezoelectric layer thickness, the electric field vector in each layer is reduced to a scalar component given by

$$E_{zi} = -\frac{\phi_i}{t_i} \tag{9}$$

#### 2.3 Variation Formulation

The principle of stationary potential energy states that the equilibrium state is the one where the potential energy is stationary, and can be mathematically written as

$$\delta U + \delta V = 0 \tag{10}$$

where U is the potential energy of the system and V is the negative of the work done by external forces.

The potential energy is given by

$$U = \frac{1}{2} \int_{V_T} \{ \boldsymbol{\varepsilon} \}^T \left[ \bar{Q} \right] \{ \boldsymbol{\varepsilon} \} dV - \int_{V_p} \{ \boldsymbol{\varepsilon} \}^T \left[ e \right] \{ E \} dV - \frac{1}{2} \int_{V_p} \{ E \}^T \left[ \boldsymbol{\varepsilon} \right] \{ E \} dV$$
(11)

where  $V_T$  is the total volume of the beam and  $V_P$  are the piezoelectric layers volume. In Equation (11) the first term is the strain energy stored in the elastic continuum, the second term is a coupling energy that transfer energy between the electrical and mechanical domain, and the last term is the electric energy stored in the piezoelectric layers.

Considering  $\{\varepsilon\} = \{\varepsilon_{xx} \quad \gamma_{xz}\}^T$  and  $\{E\} = E_z$ , the matrices  $[\bar{Q}], [e]$  and  $[\varepsilon]$  are reduced to a  $2 \times 2$ ,  $2 \times 1$  and  $1 \times 1$  matrix, respectively. Let

$$\{q\} = \left\{ \begin{array}{c} \{u\} \\ \{w\} \\ \{\theta\} \\ \{\phi^S\} \end{array} \right\}$$
 (12)

be the vector of independent variables consisting of nodal displacements and sensors electric potentials. Substituting Equations 4 and 8 into Equation 11, and rewriting using Equation 12 the first variation of U is given by

$$\delta U = \{\delta q\}^T [K_{nl}] \{q\} = \{\delta q\}^T \{F_{int}\}$$
 (13)

where  $[K_{nl}]$  is the nonlinear stiffness matrix, which is a quadratic function of the independent variables. This matrix is fully populated and can be divided into sub-matrices as

$$[K_{nl}] = \begin{bmatrix} [K_{uu}] & [K_{uw}] & [K_{u\theta}] & [K_{u\phi}] \\ [K_{wu}] & [K_{ww}] & [K_{w\theta}] & [K_{w\phi}] \\ [K_{\theta u}] & [K_{\theta w}] & [K_{\theta \theta}] & [K_{\theta \phi}] \\ [K_{\phi u}] & [K_{\phi w}] & [K_{\phi \theta}] & [K_{\phi \phi}] \end{bmatrix}$$

$$(14)$$

Let  $F_u$ ,  $F_w$ ,  $F_\theta$  and  $F_\phi$  be external nodal loads applied to the axial, transversal, rotational and electric DOFs, respectively. Taking

the first variation of the work performed by external loads, the second term in the right-hand side in Equation 10 can expressed as

$$\delta V = -\{\delta q\}^T \{F_{ext}\} \tag{15}$$

where the external forcing vector is

$$\{F_{ext}\} = \left\{ \begin{array}{l} F_{u} - \left[K_{u\phi}^{A}\right] \{\phi^{A}\} \\ F_{w} - \left[K_{w\phi}^{A}\right] \{\phi^{A}\} \\ F_{\theta} - \left[K_{\theta\phi}^{A}\right] \{\phi^{A}\} \\ F_{\phi} \end{array} \right\}$$
(16)

Substituting Equations 13 and 15 into Equation 10, one gets

$$\delta U + \delta V = \{\delta q\}^T (\{F_{int}\} - \{F_{ext}\}) = 0$$
 (17)

For any arbitrary and admissible variation in the independent variables vector,  $\{\delta q\} \neq 0$ , Equation 17 can be rewritten as

$$\{F_{int}\} - \{F_{ext}\} = \{0\}$$
 (18)

#### 3 Solution Method

The Arc Length Method [13] is a highly efficient numerical technique used to solve strongly nonlinear set of equations, which exhibits one or more points where the tangent stiffness matrix is singular. Implementation of the Arc Length Method starts with the statement of equilibrium as

$$\{g\} = \{F_{int}\} - \lambda\{\bar{F}\} = \{0\}$$
 (19)

where  $\{g\}$  is the out-of-balance force vector that is a function of the scalar load multiplier,  $\lambda$ , and the independent variables,  $\{q\}$ . Equation 19 has m+1 variables and only m equations, making it an undetermined system that needs an additional equation to be solved. The remaining relationship between displacements, voltages and load factor comes in the form a constraint equation, given in incremental form by [14]

$$a = \{\Delta q\}^T \{\Delta q\} + \Delta \lambda^2 \Psi^2 \{\bar{F}\}^T \{\bar{F}\} - \Delta l^2 = 0$$
(20)

where  $\Psi$  is the scale factor and  $\Delta l$  is the predefined size of desired intersection, which approximates the arc length and defines the maximum search radius in the hyper-plane formed by the unknown variables including the scalar load multiplier.

Expanding Equations 19 and 20 into a Taylor series where only the linear terms are kept gives

$$\{g\}_n = \{g\}_{n-1} + [K_t]_{n-1} \{\delta q\}_{n-1} - \{\bar{F}\}_{n-1} \delta \lambda_{n-1}$$

$$a_{n} = a_{n-1} + 2\{\Delta q\}_{n-1}^{T} \{\delta q\}_{n-1} + 2\Delta \lambda_{n-1} \delta \lambda_{n-1} \Psi^{2} \{\bar{F}\}^{T} \{\bar{F}\}$$
 (21)

where  $[K_t]$  is the tangent stiffness matrix and is the Jacobian of the out-of-balance force vector. By equating both expressions of Equation 21 to zero and performing some algebraic manipulations, the corrections of each interaction are found and used to update the displacements, voltages and load factor

$$\{q\}_{n} = \{q\}_{n-1} + \{\delta\bar{q}\}_{n-1} + \delta\lambda_{n-1}\{\delta q_{t}\}$$
$$\lambda_{n} = \lambda_{n-1} + \delta\lambda_{n-1} \tag{22}$$

The correction iterations are repeated until a predetermined tolerance is achieved, and the entire loop is performed again until the desired number of load factor increments. The approach discussed in this section is chosen over the conventional Newton-Raphson methods to solve the equilibrium problem because it can be used in nonlinear problems where the equilibrium path required the applied load to be decreased.

#### 4 Results

A Matlab® code was implemented to solve the equilibrium problem. In order to demonstrate the performance of the developed model, a few simulations will be carried out. The influence of stacking sequence on the electromechanical structural behavior and the effect of changing the number of actuator layers in the laminate are investigated.

Data used in simulations can be seen in Table 1, where the material properties for the T300/976 graphite/epoxy composite and PZT-G1195N piezoelectric ceramic, and geometric properties for the beam are specified, respectively.

**Table 1**: Geometric and material properties used in simulations

	T300/976	PZT-G1195N	Unit
$\overline{L}$	300	300	mm
b	40	40	mm
t	2.4	0.2	mm
$E_{11}$	150.0	63.0	GPa
$E_{22}$	9.0	63.0	GPa
$G_{13}$	7.1	24.2	GPa
$\nu_{12}$	0.30	0.30	_
<i>e</i> <sub>31</sub>	_	16.00	$C/m^2$
$\epsilon_{33}$	_	10.935	nF/m

In the actuators analyses, the voltage magnitude across each piezoelectric layer of a cantilever beam,  $\phi^A$ , is varied and the tip transversal displacement, w(L), is measured. Therefore, the electric potential applied across each pair of actuators is given by  $2\phi^A$ . For the sensors simulations, the magnitude of a transversal tip load on a cantilever beam, P, is varied and the tip displacement and average voltage across the elements,  $\phi^S$ , are measured. Both configurations can be seen on Fig. 7.

# 4.1 Stacking Sequence Variation

To verify the influence of stacking sequence on the electromechanical behavior of actuator and sensors, five different symmetric laminates were compared. The first stacking sequence is  $[p/-45/45]_s$ , where the entry 'p' denotes that these layers have piezoelectric properties, and is chosen as reference. The others are  $[p/0/0]_s$ ,

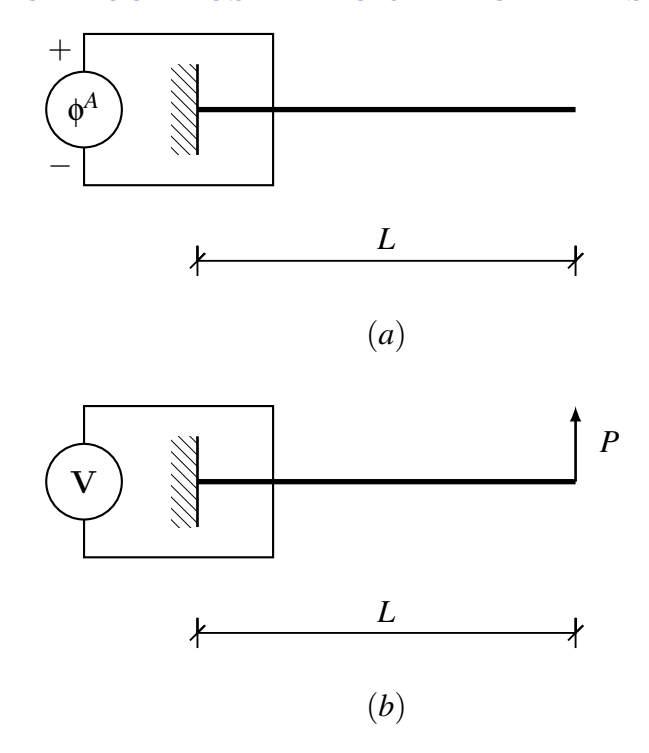


Fig. 7: Cantilever beam used in simulations: (a) actuator configuration; and (b) sensor configuration.

 $[p/-30/60]_s$ ,  $[p/-90/90]_s$  and  $[p/90/0]_s$ . Geometric and material properties can be found on Table 1.

The actuator behavior of different stacking sequences can be seen on Fig. 8. The sequences  $[p/0/0]_s$  and  $[p/-30/60]_s$  are stiffer than the reference needing higher voltage levels to achieve the same displacement, while the sequences  $[p/-90/90]_s$  and  $[p/90/0]_s$  are more flexible than the baseline needing a lower voltage in the piezoelectric actuators to achieve the same tip displacement. The sequence  $[p/0/0]_s$  is the most rigid because all graphite fibers are aligned with the axial direction leading to a fiber predominant material property, while the sequence  $[p/-90/90]_s$ is the most flexible due to the fibers being aligned with the transverse direction, which results in an epoxy matrix predominant material property. The ratio  $\frac{E_{11}}{E_{22}}$  is 16.667 and explains the difference between the two extreme cases.

A similar analysis is valid for the sensor

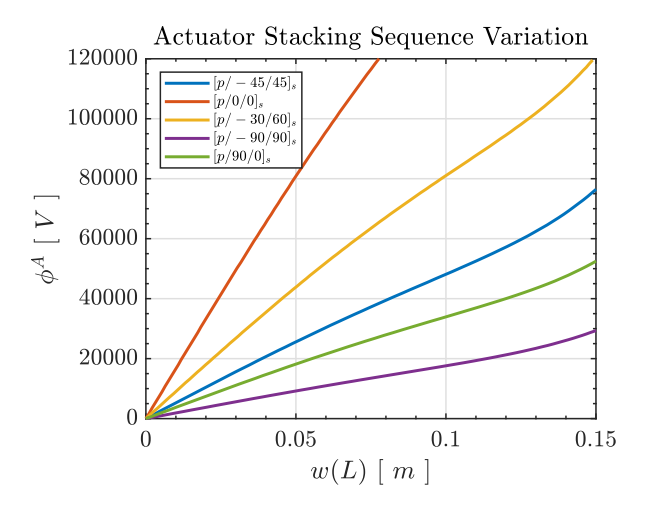


Fig. 8: Stacking sequence variation on an actuator bimorph beam.

operational mode, and is shown on Fig. 9 and Fig. 10. For a predetermined tip load, the stacking sequence  $[p/0/0]_s$  has the lowest displacement, which leads to a lower sensing voltage across the piezoelectric layers. The sequence  $[p/-90/90]_s$ , however, yields the highest tip displacement and, consequently, the higher electric potential.

This case study shows that composite structures are versatile and the stacking sequence is extremely important to define its behavior under electrical or mechanical external loads. For the case where piezoelectric layers work as actuators, it is desired that the beam exhibits a certain level of flexibility allowing the element to morph at lower applied voltage levels; however, this suggestion is relative to the actuation mechanism only, and another requirements such as the ones regarding structural strength, manufacturing process and aeroeleasticity should be taken into account when applying this kind of smart structures into real aircrafts. When the piezoelectric layers act as sensors, no design guideline are recommended since the element is passive and used to monitor the structural behavior.

# 4.2 Number of Actuator Layers

This analysis considers a laminate with twenty two layers with varying number of actuators.

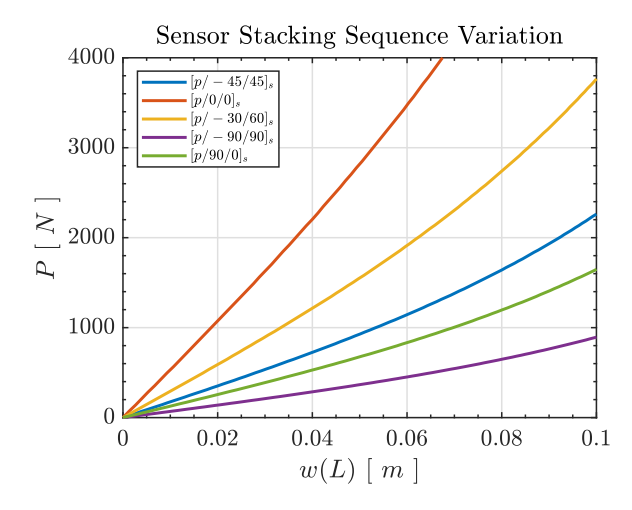


Fig. 9: Stacking sequence variation on a sensor bimorph beam. Load versus tip displacement.

The thickness of all layers are considered to be t=0.2mm, while the other properties are the ones in Table 1. The reference stacking sequence, with two piezoelectric layers, is  $[p/45/-45/35/45/-45/-35/0_2/90_2]_s$ . The ply orientations 35 and -35 were chosen in order to maintain equal Young's Modulus values for the composite and piezoelectric materials, assuring that the structure has the same stiffness. Four and six actuator layers, with stacking sequences  $[p/45/-45/p/45/-45/p/0_2/90_2]_s$  for the first and  $[p/45/-45/p/45/-45/p/0_2/90_2]_s$  for the latter, were used in the comparison.

The results are shown on Fig. 11. The top and bottom layers were subjected to opposite sign electric potential of the same intensity,  $\phi^A$ , and the tip displacement were measured. For a fixed displacement, the higher the number of actuators, the lower is the voltage applied in each piezoelectric layer. This behavior was expected since for each additional pair of actuators, more energy is introduced on the system and is converted in mechanical strain. Thus, to efficiently design an active piezoelectric beam, one can embed various actuating layers within the structure, decreasing the electric potential magnitude used to enforce deformation.

# AN ACTIVE-PASSIVE NONLINEAR FINITE ELEMENT MODEL FOR ELECTROMECHANICAL COMPOSITE MORPHING BEAMS

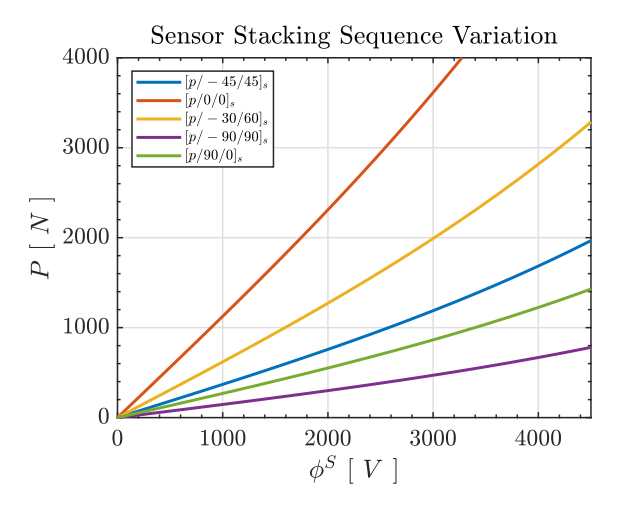


Fig. 10: Stacking sequence variation on a sensor bimorph beam. Load versus average voltage across layers.

#### 5 Conclusion

A finite element formulation for geometrically nonlinear composite morphing beams with embedded piezoelectric layers was derived. Each lamina can be of different materials, with piezoelectric characteristics or not, and the number of actuators and sensors are predefined. Classical laminate theory accounts for each layer's orientation with respect to the beam longitudinal axis and the material properties which varies across the thickness. The piezoelectric effect was modeled using a linear approximation, where all electromechanical layers are polarized in the thickness direction. Geometric nonlinearities are added using the complete Green strain tensor, which is a set of nonlinear partial differential equations which measures the degree of deformation on a body. The kinematic assumptions are the ones stated on Timoshenko's beam theory, in which cross-sections are no longer perpendicular do the neutral plane.

The addition of nonlinear terms in the element formulation introduces a hardening effect in the structural behavior, with the linear formulations underestimating the response when both models are subjected to the same level of input. This assumptions also leads to a full coupled stiffness

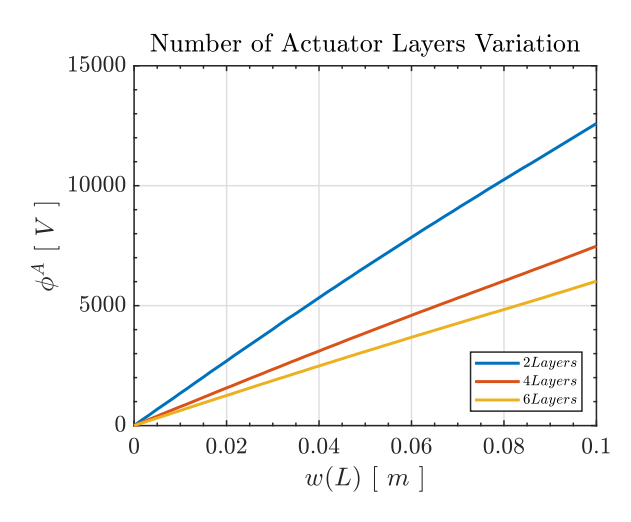


Fig. 11: Number of actuator layers variation.

matrix, with membrane-bending, membranerotation, bending-rotation and mechanicalelectrical coupling.

Simulations have shown that the stacking sequence is of great importance in the structure behavior, and a beam with the same number of layers and material can exhibit different electromechanical behavior depending only in the orientation of fibers. For morphing actuators beams, the best stacking sequence, when only morphing requirements are being considered, is the one that provides lower stiffness in order to allow the structure to change shape with a lower voltage. Increasing the number of actuators also contributes to lowering the voltage needed to morph the element, and the adequate piezoelectric material should be chosen when designing morphing beams.

### References

- Seigler T, Neal D, Bae J and Inman D. Modeling and flight control of large-scale morphing aircraft. *Journal of Aircraft*, Vol. 44, No. 4, pp 1077, 2007.
- [2] Ajaj R, Beaverstock C and Friswell M. Morphing aircraft: the need for a new design philosophy. Aerospace Science and Technology, Vol. 49, pp 154-166, 2016.
- [3] Bilgen O, Kochersberger K, Diggs E, Kurdila A and Inman D. Morphing wing micro-air-vehicles via macro-fiber-

- composite actuators. Proceedings of the 48th AIAA/ASME/ASCE/AHS/ASC Structures, Structural Dynamics, and Materials Conference, 2007.
- [4] Usher T, Ulibarri K and Camargo G. Piezoelectric microfiber composite actuators for morphing wings. ISRN Materials Science, 2013.
- [5] Ofori-Atta K. Morphing wings using macro fiber composites. *McNair Scholars Research Journal*, Vol. 1, No. 1, 2014.
- [6] Kim J, Grisso B, Kim J, Ha D and Inman D. Electrical modeling of piezoelectric ceramics for analysis and evaluation of sensory systems. Sensors Applications Symposium, 2008. SAS 2008. IEEE, pp 122-127, 2008.
- [7] Crawley E and de Luis J. Use of piezoelectric actuators as elements of intelligent structures. *AIAA journal*, Vol. 25, No. 10, pp 1373-1385, 1987.
- [8] Benjeddou A. Advances in piezoelectric finite element modeling of adaptive structural elements: a survey. *Computers & Structures*, Vol. 76, No. 1, pp 347-363, 2000.
- [9] Wang G. Analysis of bimorph piezoelectric beam energy harvesters using Timoshenko and Euler-Bernoulli beam theory. *Journal of Intelligent Material Systems and Structures*, Vol. 24, No. 2, pp 226-239, 2013.
- [10] Kusculuoglu Z, Fallahi B and Royston T. Finite element model of a beam with a piezoceramic patch actuator. *Journal of Sound and Vibration*, Vol. 276, No. 1, pp 27-44, 2004.
- [11] Alaimo A, Milazzo A and Orlando C. A smart composite-piezoelectric onedimensional finite element model for vibration damping analysis. *Journal of Intelligent Material Systems and Structures*, Vol. 27, No. 10, pp 1362-1375, 2016.
- [12] Cardoso E and Fonseca J. An incremental lagrangian formulation to the analysis of piezoelectric bodies subjected to geometric nonlinearities. *International Journal for Numerical Methods in Engineering*, Vol. 59, No. 7, pp 963-987, 2004.
- [13] Riks E. An incremental approach to the solution of snapping and buckling problems.

- Journal of Solid Structures, Vol. 15, pp 529-551, 1979.
- [14] Crisfield M. Non-linear finite element analysis of solids and structures. 1st edition, John Wiley and Sons, 1996.

### **Contact Author Email Address**

mailto: raul.olympio@embraer.com.br

## Copyright Statement

The authors confirm that they, and/or their company or organization, hold copyright on all of the original material included in this paper. The authors also confirm that they have obtained permission, from the copyright holder of any third party material included in this paper, to publish it as part of their paper. The authors confirm that they give permission, or have obtained permission from the copyright holder of this paper, for the publication and distribution of this paper as part of the ICAS proceedings or as individual off-prints from the proceedings.